Desalination and Water Treatment
www.deswater.com

51 (2013) 863–871
January

Taylor & Francis
Taylor & Francis Group

doi: 10.1080/19443994.2012.714097

Effect of fixed bed characteristics on the performance of pulsed water flow humidification-dehumidification solar desalination unit

A.H. El-Shazly[a,b,*], A.A. Al-Zahrani[a,b], Y.A. Al-Hamed[a,b], S.A. Nosier[a,b]

[a]*Chemical and Materials Engineering Department, Faculty of Engineering, King Abdulaziz University, Jeddah, Saudi Arabia*
Email: aalshazly@kau.edu.sa
[b]*Center of Excellence in Desalination Technology, King Abdulaziz University, Jeddah, Saudi Arabia*

Received 17 March 2012; Accepted 17 July 2012

ABSTRACT

This work investigates the effect of fixed bed characteristics on the performance a of pulsed flow humidification-dehumidification (HD) solar desalination unit. The results show that the unit performance has been improved by increasing the Raschig ring diameter and increasing the distance between layers up to a certain limit and by decreasing the bed height. The solar collector located in Jeddah Saudi Arabia was investigated under different conditions of feed water flow rate, tilt angle, and area of the collector. An equation for the collector efficiency and performance was derived. The power loss in the condenser was calculated to be 2.125 W. The results showed that the productivity of the unit within the range of data studied can be within the range from 1.3 to 1.9 $l/m^2 \cdot h$ and the gain output ratio of the pulsed flow system to be within the range of 1.80–2.74.

Keywords: Pulsed flow; Desalination; Humidification-dehumidification; Solar collector; Fixed bed; Mass transfer

1. Introduction

The technology of humidification-dehumidification (HD) satisfies some of the desalination demands, in particular flexibility in capacity with moderate installation and operating costs. The current HD installations are in very compact units containing two exchangers: an evaporator where air is humidified and a condenser where distilled water is recovered. Many devices are used for air humidification including spray towers, bubble columns, wetted-wall towers and packed bed towers [1–4]. The driving force for this diffusion process is the concentration difference between the water-air interface and the water vapor in air. This concentration difference depends on the vapor pressure at the gas-liquid interface and the partial pressure of water vapor in the air. Spray towers have received most of the investigators attention as they are simple in design and have minimal pressure drop on the gas side. However these towers have high capacity but low efficiency as a result of the low water holdup due to the loose packing flow [2]. Younis et al. [2] and Ben-Amara et al. [3] used a spray tower as the humidifier in their HD systems and they found that increasing the amount of water sprayed increased the absolute outlet humidity. However, further increase in the water quantity

*Corresponding author.

Presented at the International Conference on Desalination for the Environment, Clean Water and Energy, European Desalination Society, 23–26 April 2012, Barcelona, Spain

resulted in air cooling and this condenses some of the water vapor content in the air. This means a decrease in the absolute humidity, although the outlet air is always saturated. Therefore, for air heated HD cycles there is an optimum value of the mass flow ratio which gives maximum air humidity. This fact promotes the use of multi-stage air heater and humidifier combinations to increase the fresh water production. The application of pulsation or reciprocation has been recognized as an effective process intensification technique that enhances mass and heat transfer rates, and improves both process productivity and product quality [5–10]. Different studies have presented experimental, analytical and numerical investigations on the effect of pulsation on heat transfer characteristics [11–18]. Habib et al. [19] investigated the characteristic of laminar pulsating flow inside the tube under uniform wall heat flux experimentally at different frequencies from 6.6 to 68 Hz. It is reported that an increase and reduction in Nusselt number are observed, depending on the values of both the frequency and Reynolds number. An investigation on pulsating flow pipe with different amplitudes was carried out by Guo and Sung [20]. The results show that for the case of small amplitudes, the heat transfer coefficient can be increased or decreased depending on the pulsation frequency. However, with large amplitudes, the heat transfer rates are always enhanced. An analytical study on laminar pulsating flow in a pipe by Faghri et al. [21] reported that higher heat transfer rates are produced. They related that to the interaction between the velocity and temperature oscillation. Hemeada et al. [22] found that the overall heat transfer coefficient in laminar incompressible pulsating flow increases with increasing the amplitude and decreases with increasing the frequency and Prandtl number. The results of different investigations show that in the thermally fully developed flow region, a reduction of the local Nusselt number was observed with pulsation of small amplitude. However, with large amplitude, an increase in the value of Nusselt number was noticed. In summary, the time average Nusselt number of a laminar pulsating internal flow may be higher or lower than that of the steady flow one, depending on the frequency. Recently, it was shown that more than 20-fold increase in the mass transfer rate could be achieved by vibrating vertical electrodes along their length [23–26]. Among its applications in that field are electrochemical processing, electroplating, metal recovery from bio-leaching solutions, and more recently the manufacture of Printed Wiring Board [27–30]. In all of the above mentioned applications, generation of an oscillatory field at the solid–liquid interface is achieved by vibrating either the solid surface or the fluid surrounding it. Although both approaches achieve the same objective, the former is more energy efficient since the energy dissipation there is mainly focused in the boundary layer adjacent to the solid–liquid interface rather than in the bulk of the fluid medium. When the power needed to vibrate the electrode was taken into consideration, Al-Taweel and Ismail [30] found that both amplitude and frequency have almost equal effect on the enhancement obtained per unit power consumed. From the above it is clear that pulsation or vibration can be considered as a good tool for enhancing the rate of mass and/or heat transfer in the humidification process. Previous investigations by the authors [31] on the effect of pulsation on humidification unit performance showed that the unit productivity has been increased by increasing the off time i.e. decreasing the frequency of pulsed water flow up to certain levels and that increasing the amplitude of water pulsation (water flow per pulse) was found to increase the unit productivity as well.

This work investigates the effect of design parameters i.e. fixed bed characteristics on the performance of pulsed water flow humidification-dehumidification solar desalination unit.

2. Experimental setup and procedure

2.1. Experimental setup

The system is composed of three main units which are the solar collector, humidification and the dehumidification units. The solar collector was made of the flat plate type; its dimensions were about 100 cm wide, 160 cm long and 10 cm high. It consisted (Fig. 1) of an iron sheet base of 3 mm thickness; a glass wool layer of 3 cm thickness; a corrugated iron sheet; a glass cover 3 mm thick, and a 0.5 inch schedule 40 iron tube. The iron tube was 1.5 m long with one tube pass; the tubes have one inlet and exit headers. All iron sheets and tubes were painted with black dye. The solar heater

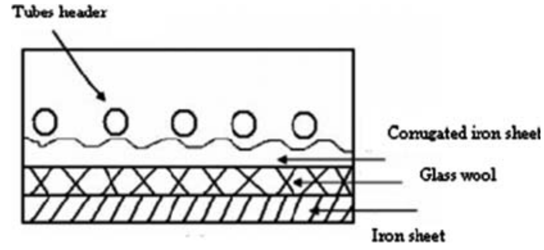

Fig. 1. Solar collector components and layers.

was positioned facing south at different tilt angles ranging from 0 to 45°.

The humidification unit Fig. 2 is a Plexiglas column of 30 cm diameter by 200 cm height, composed of three layers of plastic Raschig rings, supported on a perforated plate, the layers are separated from each others by 40 cm equal distances distributed along the column length, the layer height was fixed at 10 cm height. The hot water from the hot water storage tank was driven through the HD unit in pulsed flow regime counter current to a continuous air flow forced to the bottom of the humidifier by using a blower. Pulsation of the hot water was carried out by using a control system composed of on-off time controller, centrifugal pump and two solenoid valves, SV1 and SV2 which are working reversely. The exit water out of the humidifier was recycled back to the hot brine storage tank. The volumetric flow rate, inlet and outlet dry bulb and wet bulb temperatures, and the inlet and outlet relative humidity of air were measured by using FM1, RTD_s 1 and 2, $RTDw_s$ 1 and 2 and Hrs_s 1 and 2, respectively. For water the flow rate, inlet and outlet temperatures were measured by using FM1, RTD_s 4 and 5, respectively. In the humidification unit there is a constant water level at the bottom of the HD unit to ensure prevention of air from flowing downward through the bottom of the HD unit.

The dehumidification system (Fig. 2) is composed of three main units which are the large storage tank of 400 l capacity, the condenser, and a hot air cooler (car radiator was used) for cooling the hot water exit from the condenser. The condenser unit was composed of 130 tubes bundle, the bundle contains 13 rows with 10 columns ($N_L = 13$, $N_T = 10$), the tubes are 2.54 cm in diameter, and 60 cm in height with $S_L = S_T = 2D$. A main manifold of 2.54 cm diameter was used for

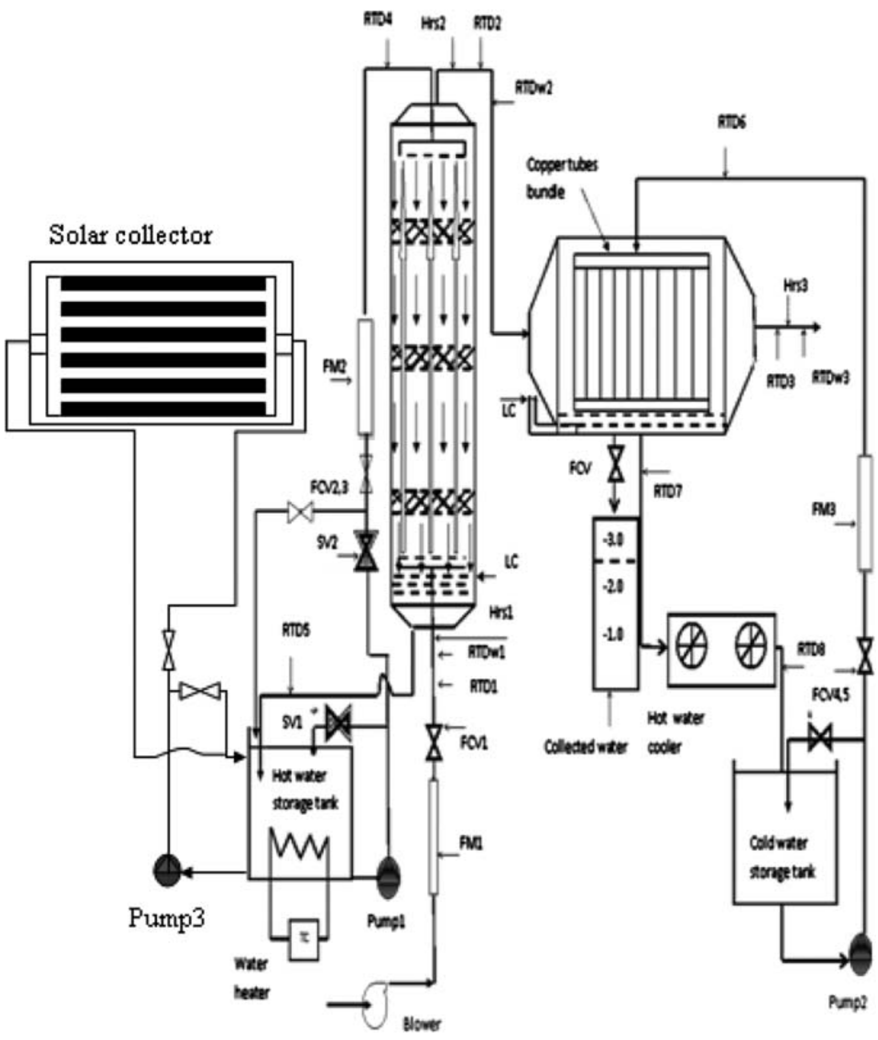

Fig. 2. Experimental setup.

supplying each row with fresh cold water i.e. the flow of cold water through tubes is of the once through one. The exit hot water from the tubes bundle collects in a main manifold to air cooler for cooling the water before being transferred to a large storage tank. Inlet and outlet temperatures of water were measured using RTD_s 6 and 7 while those for air are RTD_s 2 and 3. The inlet and outlet relative humidity and wet bulb temperatures of air in the condenser unit were measured by using Hrs_s 2 and 3 $RTDw_s$ 2 and 3, respectively. At the bottom of the condenser unit there is a constant water level for preventing air from escaping through the desalinated water collection tube, in addition there is a control valve at the bottom of the condenser which is usually closed during the dehumidification process.

2.2. Procedure

The process starts by forcing air to the bottom of the humidification unit using 1 hp blower, then hot water from the hot water storage tank starts flowing to the top of the HD unit using 0.33 hp centrifugal pump. Water was heated to a certain temperature by circulating water through the solar collector. The frequency of pulsed flow (on-off time) and the amplitude (capacity of flowing water) were adjusted to the required values by the on-off time controller connected to two solenoid valves, SV1 and SV2 and flow control valve FM2 respectively. The on time of the pulsed flow was constant at 20 s while that of the off time ranged from 20 to 60 s, different on-off combinations were investigated for its effect on the performance of the process. The capacity of pulsed water fixed at 15 l/min and controlled by a control valve FCV_s 2 and 3. The flow rate of inlet water was measured using water rotameter FM2, while temperatures of inlet and exit water were measured by using two digital thermometers RTD_s 4 and 5 fixed at the inlet and outlet lines respectively. Exit water from the HD unit is recycled back to the hot water storage tank. The exit air from the HD unit flows to the condenser where it flows in cross flow to the cooling water then exits to the atmosphere. Flow rate of air was measured by using air rotameter FM1 and fixed at 5 m^3/h. A centrifugal pump was used for forcing cooling water to the condenser with different flow rates ranging from 0.22 to 0.42 l/s. the flow rate of cooling water was measured by rotameter FM3. The exit water from the condenser was cooled first at an air cooler and finally recycled back to the cold water storage tank. At the condenser there is a constant fresh water level at the bottom of the condenser marked at level control. The collected water due to condensation was monitored with time by collection at constant time intervals in a graduated cylinder. Many variables were investigated for their effect on the unit performance such as pulsating flow characteristics (frequency and amplitude of pulsation), inlet temperatures of both feed water and air, flow rate of inlet air and water.

3. Results and discussion

3.1. Solar collector analysis

The solar collector analysis was carried out under different conditions of tilt angle, feed water flow rate, and collector area. The results in Fig. 3 show that tilt angle in the range from 20 to 25° has the highest outlet temperature from the collector (T_o) and highest collector efficiency. These results are consistent to the rule that the optimum tilt angle for the spring and autumn is the latitude −2.5°. The small deviation from the rule may be attributed to the dusty nature of atmosphere in Jeddah during spring seasons, the time of this analysis. Fig. 3 shows that the maximum output temperature is in the range from 65 to 70°C. Fig. 4 shows the solar collector efficiency distribution during the day time, the results shows that the collector efficiency decreases with the day time from 9 am to 4 pm which can be ascribed to fact that the efficiency of the collector can be calculated by the equation that [32]:

$$\eta = \eta_o - b\frac{T_{ab} - T_{amb}}{G_T}$$

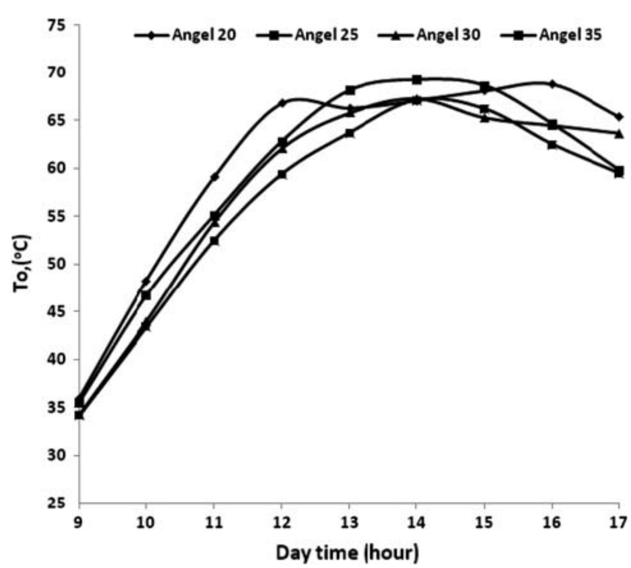

Fig. 3. Change of water output temperature with day time for different tilt angles of the collector.

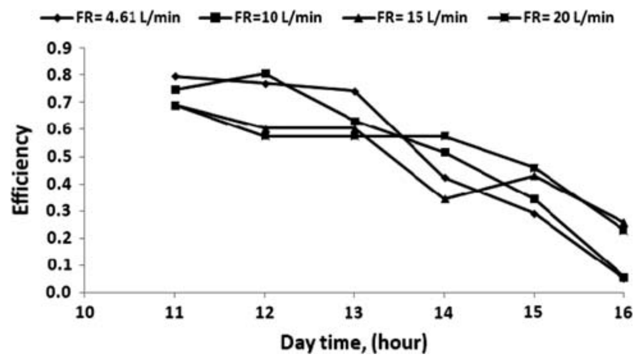

Fig. 4. Change of efficiency during the day time for different flow rates.

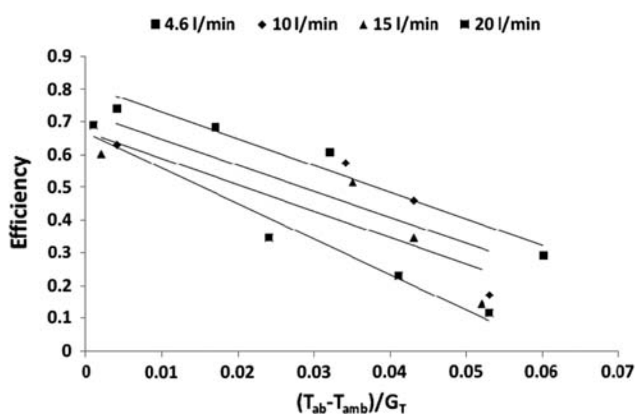

Fig. 5. Efficiency vs. $(T_{ab} - T_{amb})/G_T$ for different feed water flow rates.

where η and η_o are efficiency and the maximum efficiency of the collector respectively, T_{ab} is the average of inlet and outlet temperatures to the collector, T_{amb} is the atmospheric temperature (K) and G_T is the solar insolation rate W/m^2. At the beginning of the collector operation the value $\frac{T_{ab}-T_{amb}}{G_T}$ is the minimum and the efficiency is the highest, during the day time this value increases and the efficiency decreases. Fig. 5 shows the effect of this value $(\frac{T_{ab}-T_{amb}}{G_T})$ on the collector efficiency. Figs. 5 and 6 show the effect of feed water flow rate on the collector efficiency, it was found that the collector efficiency decreased by increasing the feed water flow rate which can be ascribed to the fact that increasing the feed water flow rate will reduce the residence time of feed water in the collector and the decrease the amount of heat gained by water which reduce the collector efficiency. The efficiency of the collector at different flow rates was derived to be in the form as shown in Table 1. The results show that η_o is the highest for lower flow rates which indicates lower heat losses from the collector in the case of lower feed rate.

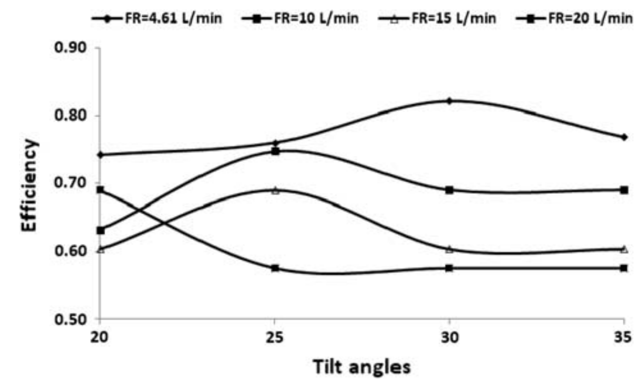

Fig. 6. Collector efficiency vs. tilt angle for different feed water flow rates.

Table 1
Solar collector efficiency for different feed water flow rate

Flow rate (l/min)	Efficiency equation
4.61	$\eta = 0.8119 - 8.1463\frac{T_{ab}-T_{amb}}{G_T}$
10	$\eta = 0.7254 - 7.9292\frac{T_{ab}-T_{amb}}{G_T}$
15	$\eta = 0.6681 - 8.041\frac{T_{ab}-T_{amb}}{G_T}$
20	$\eta = 0.6674 - 10.842\frac{T_{ab}-T_{amb}}{G_T}$

3.2. Humidification unit analysis

3.2.1. Effect of frequency of pulsation

The effect of pulses frequency was investigated by changing the off time of water flow pulsations. The results as shown in Fig. 7 show that the amount of collected water has been increased by increasing the off time up to 30 s, increasing the off time above this limit reduces the amount of collected water. The above can be ascribed to the fact that increasing the off time up to certain limit (30 s), will reduce the amount of water on the surface of Raschig rings, that

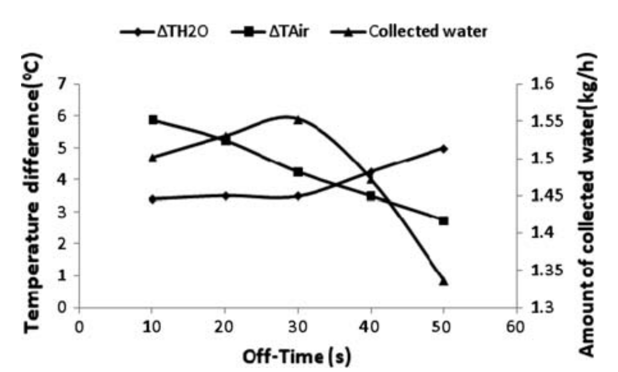

Fig. 7. Temperature difference and amount of collected water vs. off-time.

improves the agitation conditions provided by the counter upward gas flow, that reduces the thickness of the hydrodynamic boundary layer and diffusion layer between phases and that increases the mass transfer between phases and improves the unit productivity. Increasing the off time above this limit will cause dryness of the bed and reduce the amount of water vapor available to be collected which reduces the unit productivity. The above results are0 confirmed by the increase and decrease in the value of ΔT_{H_2O} and ΔT_{air} respectively that take place by increasing the off time. Increasing the off time will certainly reduce the amount of hot water supplied to the humidifier and that reduces the amount of heat available to heat the counter air flow that reduces the exit air temperature and reduces ΔT_{air}.

3.2.2. Effect of distance between layers

The results as shown in Fig. 8 show that increasing the distance between layers up to 5 cm has increased the amount of water collected. Increasing the distance between layers approximately has no effect on the unit productivity. The above results can be ascribed to fact that by increasing the distance between layers the gas agitation effect will be predominant and that reduces the thickness of diffusion layer between the gas and liquid phases. In addition the dropping of liquid from one layer to another will cause other agitation conditions and enhance the heat and mass transfer coefficients. Using one layer (i.e. distance between layers equal zero) of the bed will increase the pressure drop across the bed, and that will reduce the effect of both gas and liquid agitation conditions. The above results are consistent with the change in water and air temperature differences. Fig. 8 shows that ΔT_{H_2O} and ΔT_{air} have been increased by increasing the distance between layers which means good contact between the two phases can take place in the case of dividing the bed into layers. Increasing the distance above certain limits will reduce this effect which is ascribed to the fact that the presence of packing materials will increase the contact time between liquid and vapor phases and improve heat and mass transfer conditions.

3.2.3. Effect of packing height

Fig. 9 shows that the amounts of collected water, ΔT_{H_2O} and ΔT_{air} have been decreased by increasing the height of packed bed per layer. These results can be attributed to the damping effect of the bed height on both liquid and gas agitation effects that increase the thickness of the thermal and boundary layers which reduces both heat and mass transfer coefficients respectively.

3.2.4. Effect of Raschig ring diameter

Fig. 10 shows that the amount of collected water increased by increasing the ring diameter up to 1.27 cm (0.5 inch) while it decreased by increasing the ring diameter above this limit. The above results can be attributed to the fact that at lower ring diameters a possible damping of the eddies and disturbances that could be generated due to liquid and gas phases counter contact at the surface of Raschig rings will take place. For higher ring diameters a higher thickness of the hydrodynamic boundary layer and diffusion layer will be formed on the rings surface and that will also reduce the mass transfer coefficient between the two phases and reduce the amount of fresh water that can be produced. In between the effect of the above mentioned effects can be reduced which improves the unit performance, while for ΔT_{H_2O} and ΔT_{air} these values decrease by increasing

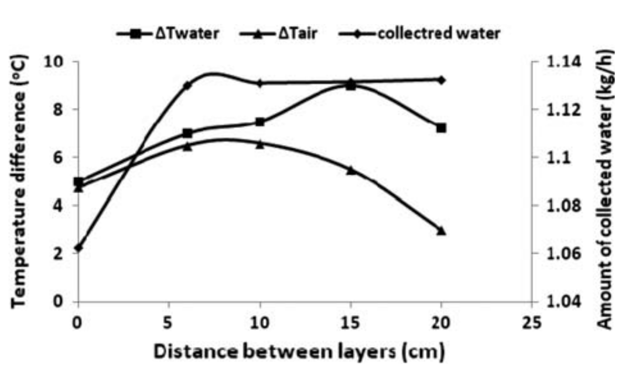

Fig. 8. Temperature difference and amount of collected water vs. distance between layers.

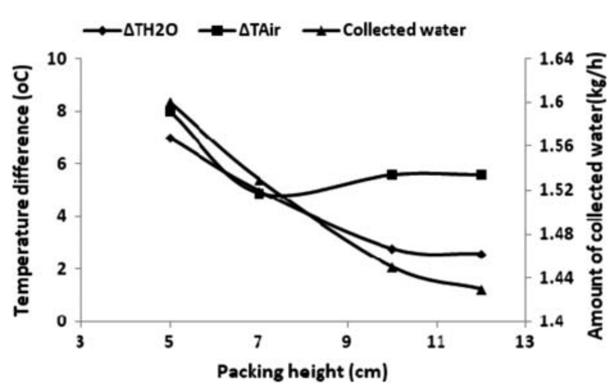

Fig. 9. Temperature difference and amount of collected water vs. packing height.

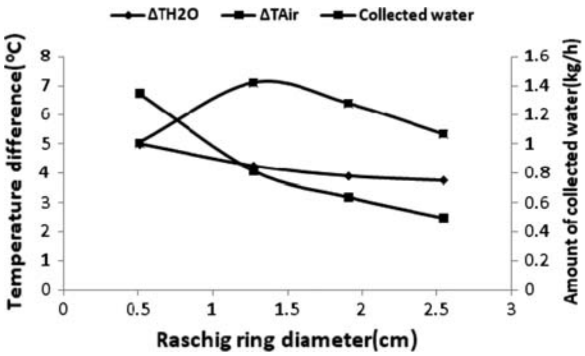

Fig. 10. Temperature difference and amount of collected water vs. Raschig ring diameter.

the ring diameter. The above results can be ascribed to that by increasing the Raschig ring diameter the bed porosity will increase and that will reduce the contact time between the liquid and gas phases and reduces the temperature elevation and reduction in gas and liquid phases respectively.

3.3. Analysis of the condenser unit

In a previous investigation by the authors of the same system [31] the performance of the condenser under different conditions of water flow rate was studied and the heat transfer coefficient was found to be 38.25 W/m·K. The tabulated data for the average overall heat transfer coefficient for finned tube heat exchanger where there is water flowing inside tubes and air in the cross flow is within the range from 25 to 50 W/m·K [33]. In this study pressure drop and power consumption through the condenser were calculated.

3.3.1. Pressure drop (ΔP) and power consumptions [33]

(A) Tube side

$$\Delta P = f\frac{\rho u_m^2}{2D}L, \quad f = \text{friction factor}$$

$$u_m = \frac{4m}{\pi D^2 \rho} = \frac{4 * 0.4845/130}{\pi * (0.0254)^2 * 997} = 7.38 * 10^{-3} \text{ m/s}$$

$$\mathrm{Re}_D = \frac{4m}{\pi D \mu} = \frac{4 * 0.4845/130}{\pi(0.0254) * 855 * 10^{-6}} = 218.6$$

for smooth laminar flow regime, $f = 0.316\ \mathrm{Re_D}^{-1/4}$ $f = 0.316\ (218.6)^{-1/4} = 0.08218$

$$\therefore \Delta P = 0.08218 * \frac{997 * (7.38 * 10^{-3})^2}{2 * 0.0254} * 0.6 = 0.0527 \text{ N/m}^2$$

$$P = \frac{\Delta P m}{\rho} = (0.0527 * 0.4845)/997 = 2.56 * 10^{-5} \text{ W}$$

(B) Shell side (air side)

For tube bundles $N_L = 13$

$$\Delta P = N_L \psi \left(\frac{\rho V_{\max}^2}{2}\right) f, \quad \psi = \text{correction factor}$$

$$V_{\max} = \left(\frac{S_T}{S_T - D}\right) * V = \left(\frac{5.08}{5.08 - 2.54}\right) * 1.016 = 2.03 \text{ m/s}$$

$$\mathrm{Re}_{D_{\max}} = \frac{V_{\max}\ D}{\gamma} = \frac{2.032 * 0.0, 254}{15.89 * 10^{-6}} = 3, 248$$

$$P_L = \frac{S_L}{D} = \frac{5.08}{2.54} = 2, \ P_T = \frac{S_T}{D} = 2, \ f = 0.22$$

$$(P_T - 1)/(P_L - 1) = \frac{2 - 1}{2 - 1} = 1.0$$

$$\psi = 1.0$$

$$\therefore \Delta P = 0.22 * 13 * 1 * \frac{1.1614 * 2.032^2}{2} = 6.857 \text{ N/m}^2$$

Mass flow rate of air through the tube bundles

$$= \rho_{air} V_{air} (N_T S_T L) = 1.1614 * 1.016 * 10 * 0.0508 * 0.6 = 0.1798 \text{ kg/s}$$

$$\text{Power} = \Delta P V_{air} = 6.857 * \frac{0.3597}{1.1614} = 2.123 \text{ W}$$

The above results show that the pressure drop due to air flow is higher than that of the water flow and that the total power required for the unit is 2.125 W.

3.4. Overall performance analysis

The solar energy will be considered as the main source of energy supply to the system. The performance of solar desalination system mainly depends on the solar radiation and environmental conditions. The gain output ratio (GOR), sometimes known as the performance ratio is a non-dimensional measure of the amount of product produced for a given heat input. Here, it is defined as [32,34]:

$$\text{GOR} = m_p.\lambda_w / Q_{in}$$

where m_p, λ_w and Q_{in} are the fresh water production rate, the heat of vaporization at the ambient conditions, and the input solar incident radiation on the solar collector field. The above results showed that the productivity of the unit within the range of data studied can be within the range from 1.3 to 1.91/m^2·h. The average intensity of solar radiation in Jeddah Saudi Arabia for spring time can be considered as up to 480 W/m^2. The above data show the GOR of the pulsed flow system to be within the range of 1.80–2.74.

4. Conclusions

This work investigates the effect of fixed bed characteristics on the performance of pulsed flow humidification-dehumidification unit (HD) solar desalination unit. Decreasing the frequency of water pulsation up to 20/30 on-off time that was found to increase the productivity of the unit. For the fixed bed characteristics the results show that the unit performance has been improved by increasing the Raschig ring diameter and increasing the distance between layers up to certain limit and by decreasing the bed height. The solar collector located in Jeddah Saudi Arabia was investigated under different conditions of feed water flow rate, tilt angle, and area of the collector. An equation for the collector efficiency performance was derived. The power loss in the condenser was calculated to be 2.125 W. The results showed that the productivity of the unit within the range of data studied can be within the range from 1.3 to 1.91/m^2.h and the GOR of the pulsed flow system to be within the range of 1.80–2.74. The above results show that using pulsed water flow with multilayer of Raschig rings fixed bed can improve the performance of the humidification dehumidification unit solar desalination units.

Nomenclature

D	—	tube diameter
DH	—	dehumidification unit
E	—	effectiveness
F	—	correction in factor
f	—	friction factor
FCV	—	flow control valve
FM	—	flow meter (rotameter)
HD	—	humidification unit
LC	—	level control
n_A	—	rate of mass transfer
N_L	—	number of rows per bundle
N_T	—	number of columns per bundle
P	—	power consumption
RTDw	—	thermometer for wet bulb temperature
RTD	—	thermometer for dry bulb temperature
Re	—	Reynolds number
Re_{Dmax}	—	Reynolds number outside condenser tubes bundle
S_L	—	longitudinal pitch
S_T	—	transverse pitch
SV	—	Solenoid valve
Sc	—	Schmidt number
T_{wi}	—	inlet water temperature to the HD unit
T_{wo}	—	outlet water temperature from the HD unit
T_{Ai}	—	inlet air temperature to the HD unit
T_{Ao}	—	outlet air temperature from the HD unit
u_m	—	average water velocity
V_{max}	—	maximum velocity of air
V	—	volumetric flow rate of air
ΔT_{H_2O}	—	temperature difference of water in the HD unit
ΔT_{air}	—	temperature difference of air in the HD unit
ΔP	—	pressure drop
ψ	—	correction factor

Acknowledgments

We would like to acknowledge the Center of Excellence in Desalination Technology (CEDT), King Abdulaziz University, Jeddah, Saudi Arabia, for supporting the execution of this work under the grant number CEDT-30-101.

References

[1] M.A. Younis, M.A. Darwish, F. Juwayhel, Experimental and theoretical study of a humidification–dehumidification desalting system, Desalination 94 (1993) 11–24.

[2] M. Ben-Amara, I. Houcine, A. Guizani, M. Maalej, Experimental study of a multiple-effect humidification solar desalination technique, Desalination 170 (2004) 209–221.

[3] S.A. El-Agouz, M. Abugderah, Experimental analysis of humidification process by air passing through seawater, Energy Conv. Manag. 49(12) (2008) 3698–3703.

[4] A.H. El-Shazly, M.M. El-Gohary, M.E. Ossman, Performance characteristics of a solar humidification dehumidification unit using packed bed of screens as the humidifier, Desalin. Water Treat. J. 16 (2010) 1–12.

[5] R.S. Alasser, H.M. Badr, H.A. Mavromatis, Heat convection from a sphere placed in an oscillating free stream, Int. J. Heat Mass Trans. 42 (1999) 1289–1304.

[6] P. Gao, W. Han Ching, M. Herrmann, C. Kwong, P.L. Yue, Photo-oxidation of a model pollutant in an oscillatory flow reactor with baffles, Chem. Eng. Sci. 58(3–6) (2003) 1013–1021.

[7] A.M. Thomas, R. Narayanan, A comparison between mass transfer in boundary and pressure driven oscillatory flow, Int. J. Heat Mass Trans. 45 (2002) 4057–4062.

[8] F.M. Mahfouz, H.M. Badr, Mixed convection from a cylinder oscillating vertically in a quiescent fluid, Int. J. Heat Mass Trans. 38(6) (2002) 477–486.

[9] T. Nishimura, N. Oka, Y. Yoshinak, K. Kunitsugu, Influence of imposed oscillatory frequency on mass transfer enhancement of grooved channels for pulsatile flow, J. Heat Mass Trans. 43 (2000) 2365–2374.

[10] F.J. Poulin, G.R. Flierl, J. Pedlosky, Parametric instability in oscillatory shear flows, J. Fluid Mech. 481 (2003) 329–353.

[11] M. Artineelli, R.C. Boeleter, L.M.K. Weinberg, S.E.B. Yakahi, Heat transfer to a fluid flowing periodical at low frequencies in a vertical tube, Trans. ASME, 65 (1943) 789–798.

[12] M.H.I. Barid, G.J. Duncan, J.I. Smith, J. Taylor, Heat transfer in pulsed turbulent flow, Chem. Eng. Sci. 21 (1996) 197–199.

[13] J. Chang, X.Y.L. Zhi, T.S. Zhaoan, Analytical study of pulsating laminar heat convection in a circular tube with constant heat flux, J. Heat Mass Transf. 47 (2004) 5297–5301.

[14] H. Chattopadhyay, F. Durst, S. Ray, Analysis of heat transfer in simultaneously developing pulsating laminar flow in a pipe with constant wall temperature, J. Heat Mass Transf. 33 (2006) 475–481.

[15] H.W. Cho, J.M. Hyun, Numerical solutions of pulsating flow and heat transfer characteristics in a pipe, Int. J. Heat Fluid Flow 4 (1990) 321–330.

[16] E. Elshafei, M. Safwat, H. Mansour, M. Sakr, Numerical study of heat transfer in pulsating turbulent air flow, ThETA 1, January 3–6, Cairo, Egypt (2007) 68.

[17] O.K. Erdal, J.L. Gainer, The effect of pulsation on heat transfer, Int. Eng. Chem. Fundam. 18(10) (1979) 11–15.

[18] M.A. Habib, A.M. Attya, S.A.M. Said, A.L. Eid, A.Z. Aly, Heat transfer characteristics and Nusselt number correlation of turbulent pulsating air flows, J. Heat Mass Transf. 40 (2004) 307–318.

[19] M.A. Habib, A.M. Attya, S.A.M. Said, A.l. Eid, A.Z. Aly, Convective heat transfer characteristics of laminar pulsating air flow, J. Heat Mass Transf. 38 (2002) 221–232.

[20] Z. Guo, H.J. Sung, Analysis of the Nusselt number in pulsating pipe flow, J. Heat Mass Transf. 40(10) (1997) 2486–2489.

[21] M. Faghri, K. Javdani, A. Faghri, Heat transfer with laminar pulsating flow in pipe, Lett. Heat Mass Transf. 6(4) (1979) 259–270.

[22] H. Hemeada, M.N. Sabry, A. AbdelRahim, H. Mansour, Theoretical analysis of heat transfer in laminar pulsating flow, J. Heat Mass Transf. 45 (2002) 1767–1780.

[23] H.G. Gomaa, A.M. Al-Taweel, J. Landau, Mass transfer enhancement at vertically oscillating electrodes, Chem. Eng. J. 97 (2003) 141–149.

[24] A.A. Mubarak, A.H. El-Shazly, A.H. Konsowa, Recovery of copper from industrial waste solution by cementation on reciprocating horizontal perforated Zinc disc, Desalination 167 (2004) 127–133.

[25] A.H. El-Shazly, Intensification of the rate of heavy metal removal from industrial effluents by cementation on a reciprocating array of vertical parallel plates, Alex. Eng. J. 44(5) (2005) 797.

[26] A.H. El-Shazly, A.A. Mubarak, H.S. Bamufleh, Improving the diffusion controlled cementation of cadmium ions using reciprocating fixed bed of zinc rings, Defect Diffus. Forum 312–315 (2011) 694–699.

[27] P. Venkateswarlu, N. Jaya Raj, D. Subba Rao, T. Subbaiah, Mass transfer conditions on a perforated electrode support vibrating in an electrolytic cell, Chem. Eng. Process. 41 (2002) 349–356.

[28] N.G. Carpenter, E.P.L. Roberts, Mass transport and residence time characteristics of an oscillatory flow electrochemical reactor, Trans. Inst. Chem. Eng. 77 (Part A) (1999) 212–217.

[29] A.M. Al Taweel, M.I. Ismail, Comparative analysis of mass transfer at vibrating electrodes, J. Appl. Electrochem. 6 (1976) 559–564.

[30] A.H. El-Shazly, S.A. Nosier, M.Z. Al-Abd, G.H. Sedahmed, Solid liquid mass transfer at an oscillating packed bed of Raschig rings, Ind. Eng. Chem. Res. 41 (2002) 5516–5522.

[31] A.H. El-Shazly, A.A. Al-Zahrani, Y.A. Al-Hamed, S.A. Nosier, Productivity intensification of humidification dehumidification desalination unit by using pulsed water flow regime, Desalination (2012). doi:10.1016/j.desal.2012.02.023.

[32] S. Parekh, M.M. Farid, J.R. Selman, S. Al-Hallaj, Solar desalination with a humidification-dehumidification technique—a comprehensive technical review, Desalination 160 (2004) 167–186.

[33] F.P. Incropera, D.P. Dewitt, T.L. Bergman, A.S. Lavine, Fundamentals of Heat and Mass Transfer, 6th ed., Wiley, Hoboken, NJ, 2007.

[34] G. Yuan, Z. Wang, H. Li, X. Li, Experimental study of a solar desalination system based on humidification–dehumidification process, Desalination 277 (2011) 92–98.